available at www.sciencedirect.com

ScienceDirect

journal homepage: www.elsevier.com/locate/biochempharm

Pharmacological profiling of disulfiram using human tumor cell lines and human tumor cells from patients

Malin Wickström [a,*], *Katarina Danielsson* [a], *Linda Rickardson* [a], *Joachim Gullbo* [a], *Peter Nygren* [b], *Anders Isaksson* [a], *Rolf Larsson* [a], *Henrik Lövborg* [a]

[a] *Department of Medical Sciences, Division of Clinical Pharmacology, Entrance 61, 4th floor Uppsala University Hospital, SE-75185 Uppsala, Sweden*

[b] *Department of Oncology, Radiation and Clinical Immunology, Uppsala University, SE-75185 Uppsala, Sweden*

ARTICLE INFO

Article history:
Received 14 June 2006
Accepted 21 August 2006

Keywords:
Disulfiram
Cytotoxicity
Proteasome inhibitor
Patient tumor samples
Cell lines
Apoptosis

ABSTRACT

The thiocarbamate drug disulfiram has been used for decades in the treatment of alcohol abuse. Disulfiram induces apoptosis in a number of tumor cell lines and was recently by us proposed to act as a 26S proteasome inhibitor. In this work we characterized disulfiram in vitro with regard to tumor-type specificity, possible mechanisms of action and drug resistance and cell death in human tumor cell lines and in 78 samples of tumor cells from patients using the fluorometric microculture cytotoxicity assay and the automated fluorescence-imaging microscope ArrayScan®. Disulfiram induced cytotoxicity in a biphasic pattern in both cell lines and patient tumor cells. Disulfiram induced apoptosis as measured by cell membrane permeability, nuclear fragmentation/condensation and caspase-3/7 activation using high content screening assays. For many of the cell lines tested disulfiram was active in sub-micromolar concentrations. When comparing the log IC_{50} patterns with other cytotoxic agents, disulfiram showed low correlation ($R < 0.5$) with all drugs except lactacystin ($R = 0.69$), a known proteasome inhibitor, indicating that the two substances may share mechanistic pathways. Disulfiram was more active in hematological than in solid tumor samples, but substantial activity was observed in carcinomas of the ovary and the breast and in non-small cell lung cancer. Disulfiram also displayed higher cytotoxic effect in cells from chronic lymphocytic leukemia than in normal lymphocytes ($p < 0.05$), which may indicate some tumor selectivity. These results together with large clinical experience and relatively mild side effects encourage clinical studies of disulfiram as an anti-cancer agent.

1. Introduction

The dithiocarbamate drug disulfiram has been used for decades in the treatment of alcohol abuse since it inhibits aldehyde dehydrogenase. Several laboratories have investigated the antitumor activity of disulfiram, it has been shown to induce apoptosis in a number of cell lines [1–6] as well as to reduce cell growth in glioma, lung carcinoma [7] and melanoma in mice [4]. However, the underlying mechanism has not been fully established. Disulfiram has before been shown to reduce angiogenesis [7,8], inhibit DNA topoisomerases [9] and inhibit nuclear factor κB in hepatoma [3], colorectal cancer cell lines [2] and endothelial cells [10]. The cytotoxic activity has been attributed to pro-apoptotic redox-related mitochondrial membrane permeabilization [1], zinc complexation with subsequent inhibition of Zn^{2+}-dependent

* *Corresponding author*. Tel.: +46 18 6112931; fax: +46 18 51 92 37.
E-mail address: Malin.Wickstrom@medsci.uu.se (M. Wickström).
0006-2952/$ – see front matter © 2006 Elsevier Inc. All rights reserved.
doi:10.1016/j.bcp.2006.08.016

matrix metalloproteinases [8], or Cu^{2+} complexation with inactivation of Cu/Zn superoxide dismutase [7] and consequently diminished cellular generation of reactive oxygen species. It has also been proposed that disulfiram itself has limited effect but must be in complex with Cu^{2+} to be active [11]. The NFκB inhibiting activity of the disulfiram analogue pyrrolidine dithiocarbamate (PDTC) has been attributed to its antioxidative effect and chelating properties [11,12]. PDTC has been shown to inhibit proteasomal activity in combination with copper in human breast and prostate tumor cell lines [5,6]. Recently we proposed a novel mechanism for the antitumor and NFκB inhibiting activity of disulfiram. Disulfiram and PDTC were identified as 26S proteasome inhibitors in a cell-based screening assay and the mechanism was confirmed with a NFκB translocation assay [13].

Indications of a potential tumor cell selectivity has been presented for disulfiram both for melanoma cells versus normal melanocytes [1] and for chronic lymphocytic leukemia (CLL) cells versus peripheral blood mononuclear cells [13].

In the present work we continue the characterization of disulfiram in vitro with respect to tumor-type specificity, possible mechanisms of drug resistance and cell death. This was carried out in human tumor cell lines and in primary cultures of human tumor cells from a broad spectrum of diagnoses and by use of the fluorometric microculture cytotoxicity assay (FMCA) and the automated fluorescence-imaging microscope ArrayScan®.

2. Material and methods

2.1. Cell lines

The human cancer cell line panel has been described previously [14] and consists of the sensitive parental cell lines; RPMI 8226 (myeloma), CCRF-CEM (leukemia), U937-GTB (lymphoma) and NCI-H69 (small-cell lung cancer), the drug resistant sublines 8226/Dox40 (doxorubicin resistant myeloma), 8226/LR5 (melphalan resistant myeloma), CEM/VM-1 (teniposide resistant leukemia), U937/Vcr (vincristine resistant lymphoma), H69AR (doxorubicin resistant small-cell lung cancer) and the primary resistant ACHN (renal adenocarcinoma) cell line. In addition HeLa (cervical adenocarcinoma) cell line (ATCC, Manassas, VA) and the non-malignant hTERT-RPE1 epithelial cell line (CloneTech, Paolo Alto, CA) were used. Some basic resistance characteristics of the panel, designed to represent different origin and common resistance mechanisms, are presented in Table 2.

A complete medium consisting of culture medium RPMI 1640 supplemented with 10% inactivated fetal calf serum, 2 mM glutamine, 100 μg/ml streptomycin and 100 U/ml penicillin was used for all cell lines but hTERT-RPE1 and HeLa. hTERT-RPE1 was cultured in Dulbecco's modified Eagle's medium nutrient F-12 Ham and HeLa in Eagle minimal essential medium supplemented as above and with 100 mM sodium pyruvate for the HeLa medium (all from Sigma–Aldrich Co., St. Louis, MO, USA). Cells were grown at 37 °C in a humidified atmosphere containing 5% carbon dioxide, split twice weekly and were harvested in the log-phase for experimental use.

2.2. Patient tumor samples

Tumor cells from a total of 78 patients with different tumor diagnoses were used to determine the activity of disulfiram. The samples were from acute lymphocytic leukemia (ALL; $n = 12$), acute myelocytic leukemia (AML; $n = 8$), chronic lymphocytic leukemia (CLL; $n = 8$), chronic myelocytic leukemia (CML; $n = 2$), lymphoma ($n = 14$), breast cancer ($n = 2$), colorectal cancer ($n = 7$), non-small cell lung cancer (NSCLC; $n = 7$), ovarian cancer ($n = 13$) and renal cancer ($n = 5$). The tumor samples were obtained by routine surgery, diagnostic biopsy or bone marrow/peripheral blood sampling and this sampling was approved by the ethical committee at the Uppsala University. For comparison, four preparations of normal peripheral blood mononuclear cells (PBMCs) from healthy blood donors were used.

Leukemic cells and PBMCs were isolated from bone marrow or peripheral blood by 1.007 g/ml Ficoll-Paque (Pharmacia Biotech, Uppsala) density gradient centrifugation [15]. Tumor tissue from solid samples was minced into small pieces and tumor cells were then isolated by collagenase dispersion followed by purification on Percoll (Kabi Pharmacia) density gradient centrifugation [16]. Cell viability was determined by trypan blue exclusion test and the proportion of tumor cells in the preparation was judged by inspection of May-Grunwald-Giemsa-stained cytospin preparations by a cytopathologist. Cell culture medium RPMI 1640 (supplemented as described above) was used throughout. In some cases, cells were cryopreserved in a medium containing 10% dimethylsulfoxide (DMSO, Sigma) and 90% inactivated calf serum by initial freezing for 24 h at −70 °C, followed by storage at −150 °C. Cryopreservation in this way does not affect drug sensitivity [17].

2.3. Measurement of drug activity

Disulfiram (Sigma) was dissolved in DMSO and further diluted in phosphate buffered saline (PBS; Sigma). The standard anticancer drugs were obtained from commercial sources or from NCI and dissolved according to the manufacturer's instructions. The drugs were tested in five concentrations obtained by 10-fold serial dilution and the number of experiments was at least three. The FMCA has been described in detail previously [18,19] and is based on measurement of fluorescence generated from hydrolysis of fluorescein diacetate (FDA) to fluorescein by cells with intact plasma membranes. Briefly, cell suspensions were seeded into drug-prepared plates (NUNC, Roskilde, Denmark) which then were incubated 72 h. Then the plates were washed, FDA (Sigma) was added, and after 50 min of incubation the generated fluorescence was measured at 485/520 nm in a fluorometer (Fluorostar Optima, BMG Technologies, Germany). The fluorescence is proportional to the number of cells with intact plasma membrane in the well.

Cytocentrifuge preparations were made for the patient cells from the untreated control wells to check cell identity. Quality criteria for a successful analysis included a fluorescence signal in the control wells of more than five times mean blank value, a mean coefficient of variation (CV) in the control wells and blank wells of less then 30% and more than 70% tumor cells in the cell preparation before incubation.

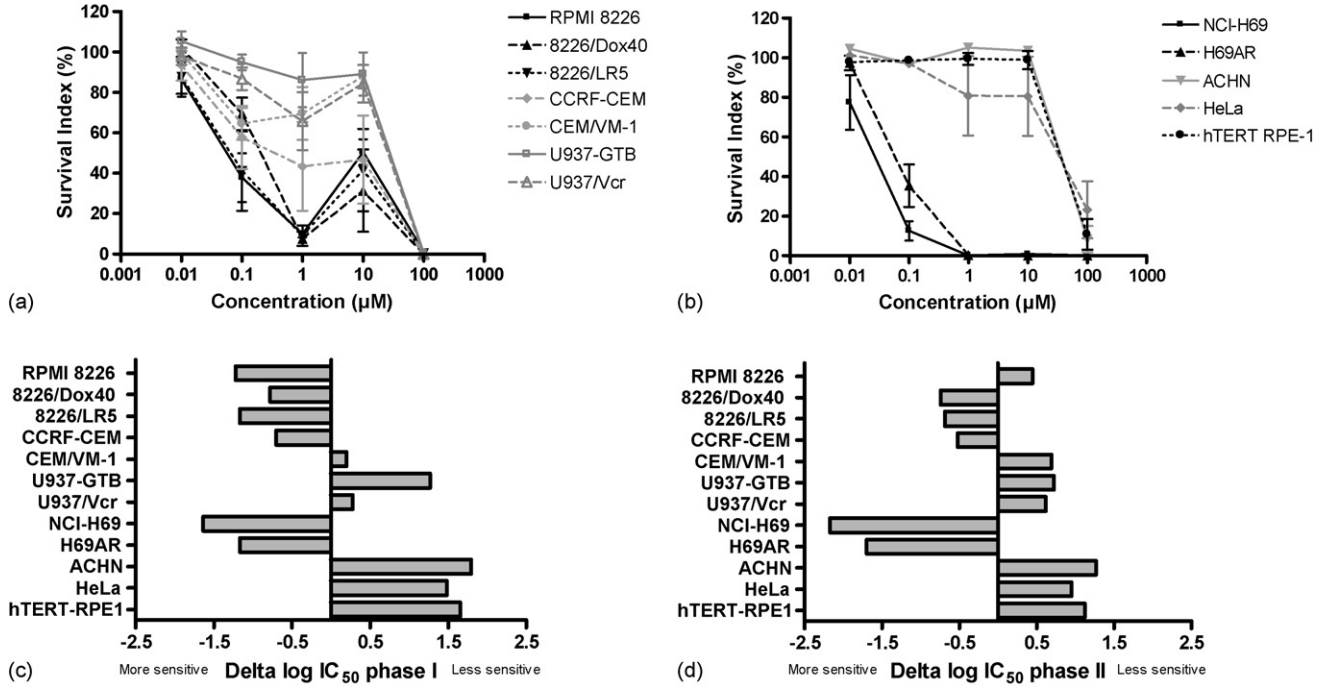

Fig. 1 – Effect of disulfiram in the 12 different cell lines as individual dose–response curves; cell lines with biphasic curves (A) and monophasic curves (B) and log IC_{50} from phase I of the dose–response curves expressed as delta (C) and log IC_{50} from phase II of the dose–response curves expressed as delta (D). Delta for a cell line was defined as the log IC_{50} for the cell line minus the mean of the log IC_{50} for all 12 cell lines. A deviation to the right and left indicates lower and higher sensitivity than the mean respectively. In A and B the results are expressed as mean values ± S.E.M., the number of experiments was at least five. The final DMSO concentration did not exceed 1% in any of the experiments. The biphasic dose–response pattern was only significant for the cell lines RPMI 8226 and CEM/VM-1 (t-test, $p < 0.05$).

2.4. *Quantification of the results from FMCA*

Cell survival is presented as survival index (SI) defined as the fluorescence in experimental wells in percent of control wells, with blank values subtracted. The IC_{50}-value (inhibitory concentration 50%) was defined as the concentration giving a SI of 50%. In some cases a biphasic dose–response curve was observed, see results. In these cases the IC_{50} was defined as the lowest concentrate reaching a SI of 50% except in Fig. 1D where second phase log IC_{50} is presented. Correlations and comparisons between IC_{50} values were performed using the logarithmic values. Comparison of activity was made with Student's *t*-tests (GraphPad Prism).

For the cell lines, a delta value was calculated as the logarithm of the IC_{50} of the individual cell line minus the mean of all 12 log IC_{50} values to visualize the cytotoxicity pattern of disulfiram in the form of a delta graph [20]. The resistance factor for disulfiram in each subline was defined as the IC_{50} of the resistant sublines divided by the IC_{50} of its sensitive parental cell line.

The solid/hematological (S/H) activity ratio was defined as the fraction responders within the solid tumor group divided by the fraction responders within the hematological tumor group. A responder was defined as a sample with an IC_{50} below the median IC_{50} for all the samples.

2.5. *Gene expression*

All cell lines were analyzed for gene expression using cDNA microarrays as described in detail previously [21]. The arrays, which contained 7458 cDNA clones included in the Human Sequence Verified Set, were obtained from Research Genetics (Huntsville, AL, USA). A complete list of genes printed on the arrays is available at: http://www.genpat.uu.se/Forskargrupper/wcn/UU/InstrAndProd_section.htm#prod. Each cell line was analyzed on two separate arrays with the dyes reversed, providing a total of four (genes printed in duplicates in each array) measurements per gene and cell line. Genes with missing values for more than half of the cell lines were removed from data set. This filter reduced the number of genes from 7458 to 3909. For genes passing this filtering criterion, an average expression level for each gene and sample was calculated and used in the analysis. Analysis was performed using $\log_2$ transformations throughout.

2.6. *Data analysis using drug and gene expression database*

The drug and gene expression databases were integrated and a correlation analysis was performed in a custom made program with similar functions as COMPARE (http://www.nci-sw.com/compare.html). Pearson's correlation coef-

ficients for all the drug–drug ($\log_{10}$ IC_{50}); gene–gene ($\log_2$) and drug–gene correlations ($\log_{10}$, $\log_2$) were automatically calculated and stored in this database. Differential drug activity and differential gene expression were displayed in delta graphs. The cell line panel's mean value was determined and subtracted from the values for each cell line to yield the variable defined as delta. Delta was subsequently used for the correlation analyses. A total of 66 drugs with known mechanism of action among them proteasome inhibitors were used in the drug–drug analysis [21].

2.7. *Multiparametric high content screening assays*

Multiparametric high content screening assays were used: Cellomics Cytotoxicity assay and an assay for measurement of apoptosis, which has been described in detail previously [22]. The HeLa cells were seeded into flat-bottomed 96-well plates (Perkin-Elmer Inc., Wellesley, MA, USA) and left to attach before addition of drugs. The number of cells seeded per well was individualized based on the proliferation rate and the optimal number of cells per well for the analysis. In the cytotoxicity assay the Multiparameter cytotoxicity HitKit™ reagents (Cellomics Inc., Pittsburgh, PA, USA) was used according to the manufacturer's instructions. Multiparameter cytotoxicity HitKit™ contains a nuclear dye, a cell permeability dye and a lysosomal mass/pH indicator. In the apoptosis assay FAM-DEVD-FMK (part of the CaspaTag Kit, Chemicon, Temecula, CA, USA) at a final concentration of 20 μM was added one hour before the end of the drug exposure to stain activated caspase-3 and partly caspase-7. The last 30 min of exposure chloromethyl-X-rosamine (MitoTracker Red CMXRos, Molecular Probes, USA) was added at the final concentration of 100 nM to evaluate mitochondrial membrane potential. The staining solutions were removed and the plates were washed twice in PBS followed by 30 min fixation with 3.7% formaldehyde and 10 μM Hoechst 33342 (Sigma), to stain nuclei. Plates were then washed twice. The plates were centrifuged before each aspiration to avoid loss of cells growing in suspension or cells detached due to toxic stimuli. Stained plates were kept at +4 °C for up to 24 h before analysis.

Plates were analyzed using the ArrayScan® high content screening system (Cellomics Inc.). The system is a computerized automated fluorescence-imaging microscope that automatically identifies stained cells and reports the intensity and distribution of fluorescence in individual cells. Images were acquired for each fluorescence channel, using suitable filters with 20X objective. In each well at least 800 cells were analyzed. Automatic focusing was performed in the nuclear channel to ensure focus regardless of staining intensities in other channels. Images and data regarding intensity and texture of the fluorescence within the individual cells, as well as the average fluorescence of the cell population within a well were stored in a Microsoft SQL database for easy retrieval and analysis.

3. Results

The dose–response curves for disulfiram in the individual cell lines are shown in Fig. 1A and B. The small cell lung carcinoma cell line NCI-H69 and its subline H69AR were most sensitive and the renal carcinoma cell line ACHN and the non-malignant epithelial cell line hTERT-RPE1 most resistant. Interestingly, the dose–responses curves from RPMI 8226/S, 8226/dox40, 8226/LR5, U937-GTB, U937/Vcr, CCRF-CEM and CEM/VM-1 were all biphasic to more or less extent, but the biphasic pattern was only significant for the cell lines RPMI 8226/S and CEM/VM-1 (t-test, $p < 0.05$). In contrast, NCI-H69, H69AR, ACHN, HeLa and hTERT-PRE1 showed significant (t-test, $p < 0.05$) monophasic growth inhibition (i.e. the next higher concentration never resulted in significant higher SI). Fig. 1C and D display delta graphs, a graphical presentation of the activity pattern of the drug in the tested panel of cell lines, i.e. the difference of log IC_{50} for each cell line from the mean log IC_{50} of the cell line panel for disulfiram. Fig. 1C shows the delta graph for log IC_{50} where the IC_{50} was defined as the lowest concentrate reaching a SI of 50%, in Fig. 1D the log IC_{50} was calculated from the second phase in those cases where a biphasic curve was occurring. Among the most sensitive cell lines were the small cell lung carcinoma NCI-H69 and the myeloma RPMI 8226 with their respective resistant sublines.

When comparing the log IC_{50} patterns with the other commonly used and experimental cytotoxic agents, disulfiram showed low correlation ($R < 0.5$) with all drugs except the proteasome inhibitor lactacystin ($R = 0.69$). The 10 drugs with highest correlation are shown in Table 1. Among them was two other known proteasome inhibitors, MG-132 and MG-262, which both showed quite low correlation ($R = 0.45$ and 0.44) with disulfiram. With the known and approved proteasome inhibitor bortezomib the correlation was almost none ($R = 0.08$). For disulfiram, the greatest difference in sensitivity between a parental line and its subline was observed for U937-GTB and U937/Vcr with a resistance factor of 0.1, indicating collateral sensitivity, and for CCRF-CEM and its resistant subline CEM/VM-1, with the resistance factor of 7.9 (Table 2). The resistance factors for some tested standard agents confirmed the expected resistance pattern of the drug resistant sublines.

In Table 3 the gene deltas with the highest positive and negative correlations (top 20) with the delta for the activity pattern of disulfiram are listed. The list includes some genes associated with drug sensitivity/resistance such as IL-4-receptor, GST, TGF-β and the members of the RAS signaling pathway.

Table 1 – The standard drugs with highest correlation

Drug	R	Mechanism of action
Lactacystin	0.69	Proteasome inhibitor
2-Azacytidine	0.46	Antimetabolite
Cisplatin	0.45	Alkylating agent
MG-132	0.45	Proteasome inhibitor
MG-262	0.44	Proteasome inhibitor
Doxorubicin	0.43	Topoisomerase I-inhibitor
6-Thioguanine	0.41	Antimetabolite
Thymidine	0.38	Antimetabolite
MGBG	0.38	Other
PALA	0.37	Antimetabolite

MGBG, methylgloxal-bis(guanylhydrazone); PALA, N-phosphoacetyl-L-aspartate.

Table 2 – Influence of resistance mechanisms on cytotoxic potency of disulfiram and standard cytotoxic agents in the cell line panel

	TopoII-associated MDR	MRP-associated MDR	Pgp-associated MDR	GSH-associated MDR	Tubulin-associated MDR
Parental celline	CCRF-CEM	NCI-H69	RPMI 8226	RPMI 8226	U937-GTB
Resistant subline	CEM/VM-1	H69AR	8226/Dox40	8226/LR-5	U937/Vcr
Resistance factor					
Disulfiram	7.9	3.0	2.8	1.1	0.10
Doxorubicin	5.6	33	43	0.61	2.0
Vincristine	1.0	27	398	1.1	61
Melphalan	1.1	0.55	3.2	3.5	1.6
Cytarabine	1.0	1.0	1.0	0.03	0.89
Cisplatin	0.71	0.89	4.7	1.1	1.4

The resistance factor was defined as the IC_{50} value in the resistant subline divided by that in its parental cell line.
TopoII, topoisomerase II; MDR, multi-drug resistance; MRP, multidrug-resistance protein; Pgp, P-glycoprotein 170; GSH, glutathione.

Table 3 – The genes with highest positive and negative correlation to disulfiram

Symbol	Acc ID	Name	R	Fold range
IL4R	714453	Interleukin 4 receptor	0.95	2.6
GHITM	727278	Growth hormone inducible transmembrane protein	0.90	3.0
EGR1	840944	Early growth response 1	0.90	2.1
MBTPS1	784504	Membrane-bound transcription factor peptidase, site 1	0.87	2.3
M6PRBP1	731356	Mannose-6-phosphate receptor binding protein 1	0.86	24
RAB32	472186	RAB32, member RAS oncogene family	0.86	5.6
CAP1	2549794	CAP, adenylate cyclase-associated protein 1 (yeast)	0.84	6.0
MT1X	297392	Metallothionein 1X	0.84	14
PHC2	898328	Polyhomeotic-like 2 (Drosophila)	0.83	4.5
LENG4	769552	Leukocyte receptor cluster (LRC) member 4	0.83	7.5
POLD4	810734	Polymerase (DNA-directed), delta 4	0.83	4.7
GSTO1	774036	Glutathione S-transferase omega 1	0.83	6.1
RIN1	725308	Ras and Rab interactor 1	0.82	3.5
SPFH1	298769	SPFH domain family, member 1	0.82	10
GOLGA3	855684	Golgi autoantigen, golgin subfamily a, 3	0.82	1.6
TGFB1	136821	Transforming growth factor, beta 1 (Camurati-Engelmann disease)	0.82	3.3
GNAI2	530139	Guanine nucleotide binding protein (G protein), alpha inhibiting activity polypeptide 2	0.82	3.2
RBPMS	343443	RNA binding protein with multiple splicing	0.81	4.3
VAMP3	843248	Vesicle-associated membrane protein 3 (cellubrevin)	0.81	3.2
DUSP3	627417	Dual specificity phosphatase 3 (vaccinia virus phosphatase VH1-related)	0.81	3.6
EXO1	447208	Exonuclease 1	−0.96	2.1
DPP3	769868	Dipeptidylpeptidase 3	−0.95	3.0
PARP1	46248	Poly (ADP-ribose) polymerase family, member 1	−0.90	14
C6orf108	504207	Chromosome 6 open reading frame 108	−0.90	2.7
EEF1E1	306921	Eukaryotic translation elongation factor 1 epsilon 1	−0.89	2.8
MEN1	685371	Multiple endocrine neoplasia I	−0.86	1.9
TM7SF2	2020772	Transmembrane 7 superfamily member 2	−0.84	5.6
	741841	Homo sapiens, clone IMAGE: 5217016, mRNA	−0.84	12
SNRPE	431803	Transcribed locus, strongly similar to NP_990581.1 SmE protein [Gallus gallus]	−0.83	2.0
KIAA0247	789232	KIAA0247	−0.83	1.6
TSNAX	740027	Translin-associated factor X	−0.82	1.4
ZNF207	246869	Zinc finger protein 207	−0.82	1.8
PRPS2	503097	Phosphoribosyl pyrophosphate synthetase 2	−0.82	1.8
UCK2	344243	Uridine-cytidine kinase 2	−0.81	3.3
FCER1G	235155	Fc fragment of IgE, high affinity I, receptor for; gamma polypeptide	−0.80	1.8
HIST1H2AE	1836558	Histone 1, H2ae	−0.80	1.7
DLG4	26021	Discs, large homolog 4 (Drosophila)	−0.80	2.9
CHD1	262996	Chromodomain helicase DNA binding protein 1	−0.80	1.6
E2F3	304908	E2F transcription factor 3	−0.80	2.1
MIG-6	742642	ERBB receptor feedback inhibitor 1	−0.79	1.9

Fold range, i.e. the expression level of the gene in cell line with highest expression divided by level in cell line with lowest level, is presented.

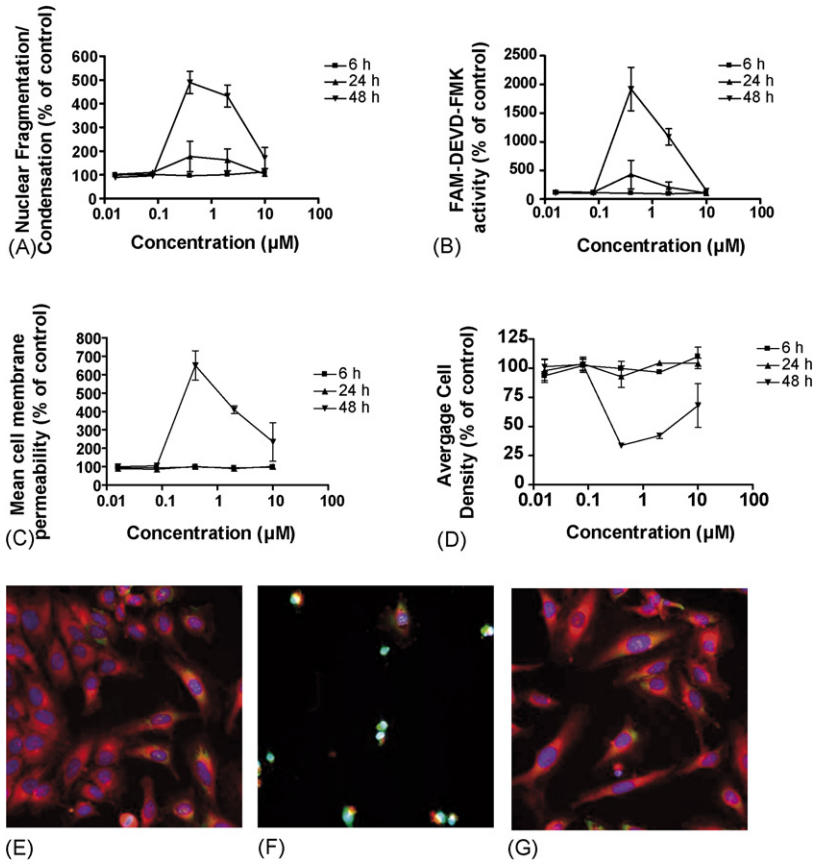

Fig. 2 – The cytotoxic effect of disulfiram over time (6–48 h) in the HeLa cell line characterized in the ArrayScan®. The nuclear fragmentation (A), caspase 3/7 activity measured using FAM-DEVD-FMK (B), mean cell permeability (C) and average cell density (D), all expressed as percent of the untreated control and averaged for at least 800 cells per well. In panel E–F composite images of HeLa cells, untreated (E), treated with 0.4 μM disulfiram for 48 h (F) and treated with 10 μM for 48 h (G). The cells were stained with 10 μM Hoechst 33342 (blue), 20 μM FAM-DEVD-FMK (green) and 100 nM MitoTracker Red CMXRos (red). Data are presented as the mean ± S.E.M. of three independent experiments. (For interpretation of the references to colour in this figure legend, the reader is referred to the web version of the article.)

As evidenced in the ArrayScan®, disulfiram caused apoptosis in HeLa cells after 48 h (Fig. 2A–G). Both DNA fragmentation/condensation and caspase-3 activation showed concentration and time dependence with a maximum at 0.4 μM after 48 h, a less pronounced effect at the same concentration after 24 h, and no effect after 6 h (Fig. 2A and B). The cell membrane permeability and cell density demonstrated the same pattern with some time delay, as no effect was seen at either 6 or 24 h (Fig. 2C and D). A reduction in mitochondrial membrane potential could be seen after 6 and 24 h (data not shown). In Fig. 2E–G images of HeLa cells exposed to disulfiram for 48 h are shown. A more marked apoptotic effect can be seen at 0.4 μM (Fig. 2F) than at 10 μM (Fig. 2G).

To measure tumor cell selectivity, drug effects in tumor cells from CLL and PBMC were compared and expressed as a ratio between the mean of the IC_{50} values of the two cell types. The ratio for disulfiram was higher than for standard agents, 2.9, the log IC_{50}s for PBMC and CLL were significantly different (*t*-test, $p < 0.05$), indicating some tumor cell selectivity (Fig. 3A). In comparison vincristine had a ratio on 2.7, but its log IC_{50}s did not significantly differ between CLL and PBMC cells, all the other standard agents had ratios below 1 (significant difference for only cytarabin, *t*-test, $p < 0.05$). The relative effect of the drugs in solid compared to hematological tumor samples, expressed as the S/H ratio, is shown in Fig. 3B. Disulfiram had an S/H ratio of 0.45 compared with 0.96 for cisplatin that had the greatest relative effect in solid tumors, consistent with its clinical use. The other drugs had considerably lower S/H ratios.

Fig. 3C displays the disulfiram sensitivity of each individual tumor sample of the ten tested cancer diagnoses tested and in PBMC. There was a large variability in IC_{50} among the lymphomas and the different solid cancer samples. As indicated by the S/H ratio disulfiram had higher activity in the hematological samples, however, disulfiram also showed good activity in ovarian cancer. Colorectal and renal cancer samples showed the least sensitive among the different tested diagnosis.

4. Discussion

Disulfiram showed cytotoxic activity in a human cell line panel as well as in tumor cells from patients with a variety of

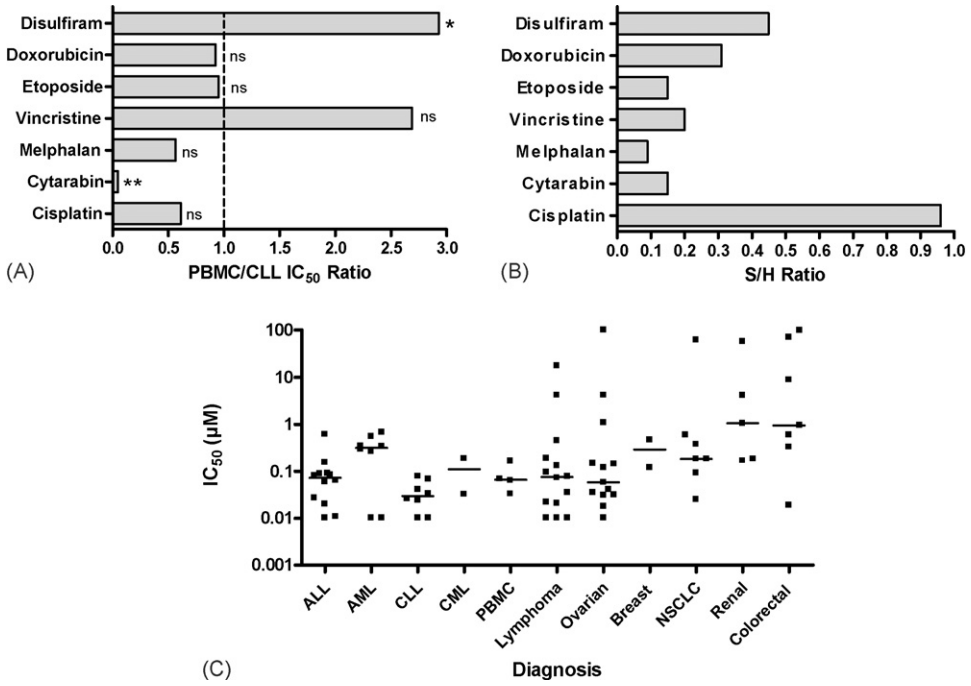

Fig. 3 – Tumor cell selectivity expressed as PBMC/CLL ratios (A) and solid/hematological (S/H) activity ratios (B) for disulfiram and some standard cytotoxic drugs in the investigated patient samples. The PBMC/CLL ratio was defined as the ratio between the geometric means of the IC_{50} values in PBMC ($n = 4$) and CLL ($n = 8$) samples. The log IC_{50}s for PBMC and CLL were significantly different for disulfiram and cytarabin (two-tailed t-test, ns = not significant, $^{*}p < 0.05$, $^{**}p < 0.01$). The S/H ratio was defined as the ratio between the fraction responders (with an IC_{50} below the median IC_{50}) within the solid and hematological tumor group. Effect of disulfiram in all individual patient samples tested, expressed as IC_{50}, with a line representing the median IC_{50} within the samples (C).

malignant diagnoses. It also induced apoptosis in a cell-based fluorescent imaging assay in HeLa cells. Cell lines are well-established models for early investigation of new anti-cancer agents, and can provide information on relevant resistance mechanisms and mechanistic similarity to other known agents [14]. Tumor cells from patients, on the other hand, provide a model that is considerably more predictive with respect to expected clinical efficacy [23].

Disulfiram has been shown to inhibit the proteasome signaling pathway [13]. Therefore it was interesting to note that among the most sensitive cell lines were the myeloma RPMI 8226 and its sublines. Multiple myeloma is the main clinical target diagnosis for bortezomib, a drug with proteasome inhibiting activity [24]. Moreover, when compared with the effect of drugs studied in the database disulfiram showed the highest (although modest in absolute amplitude) correlation with lactacystin ($R = 0.69$), a known proteasome inhibitor, further indicating that the two substances may share mechanistic pathways. However, bortezomib did not correlate at all, this has been discussed previously in Lövborg et al. [13].

Concerning the mechanisms of resistance, disulfiram seems to be sensitive to the topoisomerase II-associated multidrug resistance (resistance factor 7.9). It has been described that disulfiram inhibit DNA topoisomerase [9] that could at least to some extent explain this finding. However, the topoisomerase agents showed only modest correlations with the activity of disulfiram in the cell line panel indicating multiple determinates for disulfiram sensitivity and/or resistance.

-In the correlations analysis several genes were associated with disulfiram resistance, including IL-4 receptor, TGF-β and members of RAS signaling pathways. These genes have previously been implicated as mediators of cell survival and to prevent apoptosis [25–27]. TGF-β has previously been reported to be regulated by the proteasome system, both positively and negatively [28]. Also GST-θ and metallothionein 1 showed high correlations with disulfiram activity and the enzyme families are well known mediators of resistance to anti-cancer drugs [29,30]. However, correlation does not imply causal relationship but do provide testable hypothesizes of potential involvement of molecular pathways in determining disulfiram sensitivity.

In most of the cell lines and in many of the patient samples disulfiram displayed a biphasic cytotoxic dose–response pattern. This phenomenon has been described before for both diethyldithiocarbamate (a metabolite of disulfiram) and PDTC, regarding cell viability as well as NF κB inhibition [10,12,31–33]. The proteasome inhibiting activity of disulfiram and PDTC proposed by us is most likely accompanied by other mechanism capable of inhibiting as well as inducing cytotoxicity. The dose dependency of these, perhaps counteracting effects might explain the biphasic appearance of dose–response curves. Furthermore, attempts have been made to explain this phenomenon from different

mechanistic angles. For the disulfiram analogue PDTC it has been suggested that it inhibits monooxygenases that converts PDTC to sulphenic acid, which in turn counteracts the PDTC effect on NF κB [34]. Alternatively, high doses of PDTC might prevent the compound itself from mobilizing Zn^{2+} into intracellular compartments important for the NF κB and possibly also for the cytotoxic activity [10]. Whether the biphasic pattern of cytotoxicity is related to interference with these oxidative and metal dependent pathways or the proteasome inhibiting activity of disulfiram and PDTC needs further exploration.

The mode and time course of cell death induced by disulfiram was addressed by multiparametric apoptosis analysis. The induction of cell death was relatively slow with typical signs of apoptosis, i.e. nuclear fragmentation/condensation and activation of caspase-3, occurring after 24 h. As expected the membrane permeabilization and detachment from substrate occurred at later time points. After 48 h necrosis was induced along with apoptosis. The biphasic response seen for cytotoxicity was obvious also in these experiments. Disulfiram has previously been reported to inhibit caspases by thiol oxidation [35], which is in concordance with our data where 0.4 μM disulfiram caused more apoptosis than 10 μM. This also presents a possible mechanistic explanation for the biphasic dose–response pattern besides the ones describes above. The caspase inhibition may present a possible limiting factor in the in vivo situation, where disulfiram may inhibit the proteasome in lower doses and inhibit caspases in higher doses.

Disulfiram was more active against CLL cells compared to PBMC, indicating possible tumor selectivity. Even though disulfiram was more active in hematological than in solid tumor patient samples, the S/H ratio indicates that disulfiram may be active also in solid tumors. Disulfiram had a ratio of 0.45 that could be compared with doxorubicin, which has well known solid tumor activity, with a ratio of 0.31. According to our data, cancer of the ovary and breast would be of particular interest with respect to solid tumor activity.

Concentrations needed to induce cytotoxicity in patient hematological and some solid tumor samples can be safely reached in man [36]. Even though one needs to be careful when extrapolating in vitro results into the clinical setting, this indicates that there could be a potential for the use of disulfiram as an anti-cancer agent. The use of disulfiram in the clinic is further supported by a case report where disulfiram in combination with zinc gluconate induced clinical remission in a patient with metastatic ocular melanoma [4]. The present results together with large clinical experience and relatively mild side effects encourage future clinical studies of disulfiram in both hematological and solid tumors.

Acknowledgements

The help from Caroline Haglund, Christina Leek and Lena Lenhammar is gratefully acknowledged. This work was supported by grants from the Swedish Cancer Society, the Lions Cancer Research Fund and the Swedish Research Council.

REFERENCES

[1] Cen D, Gonzalez RI, Buckmeier JA, Kahlon RS, Tohidian NB, Meyskens Jr FL. Disulfiram induces apoptosis in human melanoma cells: a redox-related process. Mol Cancer Ther 2002;1(3):197–204.
[2] Wang W, McLeod HL, Cassidy J. Disulfiram-mediated inhibition of NF-kappaB activity enhances cytotoxicity of 5-fluorouracil in human colorectal cancer cell lines. Int J Cancer 2003;104(4):504–11.
[3] Liu GY, Frank N, Bartsch H, Lin JK. Induction of apoptosis by thiuramdisulfides, the reactive metabolites of dithiocarbamates, through coordinative modulation of NFkappaB, c-fos/c-jun, and p53 proteins. Mol Carcinog 1998;22(4):235–46.
[4] Brar SS, Grigg C, Wilson KS, Holder Jr WD, Dreau D, Austin C, et al. Disulfiram inhibits activating transcription factor/cyclic AMP-responsive element binding protein and human melanoma growth in a metal-dependent manner in vitro, in mice and in a patient with metastatic disease. Mol Cancer Ther 2004;3(9):1049–60.
[5] Chen D, Peng F, Cui QC, Daniel KG, Orlu S, Liu J, et al. Inhibition of prostate cancer cellular proteasome activity by a pyrrolidine dithiocarbamate-copper complex is associated with suppression of proliferation and induction of apoptosis. Front Biosci 2005;10:2932–9.
[6] Daniel KG, Chen D, Orlu S, Cui QC, Miller FR, Dou QP. Clioquinol and pyrrolidine dithiocarbamate complex with copper to form proteasome inhibitors and apoptosis inducers in human breast cancer cells. Breast Cancer Res 2005;7(6):897–908.
[7] Marikovsky M, Ziv V, Nevo N, Harris-Cerruti C, Mahler O. Cu/Zn superoxide dismutase plays important role in immune response. J Immunol 2003;170(6):2993–3001.
[8] Shian SG, Kao YR, Wu FY, Wu CW. Inhibition of invasion and angiogenesis by zinc-chelating agent disulfiram. Mol Pharmacol 2003;64(5):1076–84.
[9] Yakisich JS, Siden A, Eneroth P, Cruz M. Disulfiram is a potent in vitro inhibitor of DNA topoisomerases. Biochem Biophys Res Commun 2001;289(2):586–90.
[10] Kim CH, Kim JH, Moon SJ, Hsu CY, Seo JT, Ahn YS. Biphasic effects of dithiocarbamates on the activity of nuclear factor-kappaB. Eur J Pharmacol 2000;392(3):133–6.
[11] Cen D, Brayton D, Shahandeh B, Meyskens Jr FL, Farmer PJ. Disulfiram facilitates intracellular Cu uptake and induces apoptosis in human melanoma cells. J Med Chem 2004;47(27):6914–20.
[12] Schreck R, Meier B, Mannel DN, Droge W, Baeuerle PA. Dithiocarbamates as potent inhibitors of nuclear factor kappa B activation in intact cells. J Exp Med 1992;175(5):1181–94.
[13] Lövborg H, Oberg F, Rickardson L, Gullbo J, Nygren P, Larsson R. Inhibition of proteasome activity, nuclear factor-KappaB translocation and cell survival by the antialcoholism drug disulfiram. Int J Cancer 2006;118(6):1577–80.
[14] Dhar S, Nygren P, Csoka K, Botling J, Nilsson K, Larsson R. Anti-cancer drug characterisation using a human cell line panel representing defined types of drug resistance. Br J Cancer 1996;74(6):888–96.
[15] Larsson R, Kristensen J, Sandberg C, Nygren P. Laboratory determination of chemotherapeutic drug resistance in tumor cells from patients with leukemia, using a fluorometric microculture cytotoxicity assay (FMCA). Int J Cancer 1992;50(2):177–85.
[16] Csoka K, Larsson R, Tholander B, Gerdin E, de la Torre M, Nygren P. Cytotoxic drug sensitivity testing of tumor cells

from patients with ovarian carcinoma using the fluorometric microculture cytotoxicity assay (FMCA). Gynecol Oncol 1994;54(2):163–70.
[17] Nygren P, Kristensen J, Jonsson B, Sundstrom C, Lonnerholm G, Kreuger A, et al. Feasibility of the fluorometric microculture cytotoxicity assay (FMCA) for cytotoxic drug sensitivity testing of tumor cells from patients with acute lymphoblastic leukemia. Leukemia 1992;6(11):1121–8.
[18] Larsson R, Nygren P, Ekberg M, Slater L. Chemotherapeutic drug sensitivity testing of human leukemia cells in vitro using a semiautomated fluorometric assay. Leukemia 1990;4(8):567–71.
[19] Rickardson L, Fryknas M, Haglund C, Lovborg H, Nygren P, Gustafsson MG, et al. Screening of an annotated compound library for drug activity in a resistant myeloma cell line. Cancer Chemother Pharmacol 2006.
[20] Boyd MR, Paull KD. Some practical considerations and applications of the national cancer institute in vitro anticancer drug discovery screen. Drug Dev Res 1995;34(2):91–109.
[21] Rickardson L, Fryknas M, Dhar S, Lovborg H, Gullbo J, Rydaker M, et al. Identification of molecular mechanisms for cellular drug resistance by combining drug activity and gene expression profiles. Br J Cancer 2005;93(4):483–92.
[22] Lovborg H, Nygren P, Larsson R. Multiparametric evaluation of apoptosis: effects of standard cytotoxic agents and the cyanoguanidine CHS 828. Mol Cancer Ther 2004;3(5):521–6.
[23] Fridborg H, Jonsson E, Nygren P, Larsson R. Relationship between diagnosis-specific activity of cytotoxic drugs in fresh human tumour cells ex vivo and in the clinic. Eur J Cancer 1999;35(3):424–32.
[24] Adams J. The proteasome: a suitable antineoplastic target. Nat Rev Cancer 2004;4(5):349–60.
[25] Muraoka-Cook RS, Shin I, Yi JY, Easterly E, Barcellos-Hoff MH, Yingling JM, et al. Activated type I TGFbeta receptor kinase enhances the survival of mammary epithelial cells and accelerates tumor progression. Oncogene 2005.
[26] Giehl K. Oncogenic Ras in tumour progression and metastasis. Biol Chem 2005;386(3):193–205.
[27] Nowell PC, Moore JS. Aberrant responses of human lymphocytic neoplasms to cytokine regulation. Immunol Res 1998;17(1–2):171–7.
[28] Zhang F, Laiho M. On and off: proteasome and TGF-beta signaling. Exp Cell Res 2003;291(2):275–81.
[29] Balendiran GK, Dabur R, Fraser D. The role of glutathione in cancer. Cell Biochem Funct 2004;22(6):343–52.
[30] Coyle P, Philcox JC, Carey LC, Rofe AM. Metallothionein: the multipurpose protein. Cell Mol Life Sci 2002;59(4):627–47.
[31] Brennan P, O'Neill LA. 2-mercaptoethanol restores the ability of nuclear factor kappa B (NF kappa B) to bind DNA in nuclear extracts from interleukin 1-treated cells incubated with pyrollidine dithiocarbamate (PDTC). Evidence for oxidation of glutathione in the mechanism of inhibition of NF kappa B by PDTC. Biochem J 1996;320(Pt. 3):975–81.
[32] Cohen JD, Robins HI. Cytotoxicity of diethyldithiocarbamate in human versus rodent cell lines. Invest New Drugs 1990;8(2):137–42.
[33] Chung KC, Park JH, Kim CH, Lee HW, Sato N, Uchiyama Y, et al. Novel biphasic effect of pyrrolidine dithiocarbamate on neuronal cell viability is mediated by the differential regulation of intracellular zinc and copper ion levels, NF-kappaB, and MAP kinases. J Neurosci Res 2000;59(1): 117–25.
[34] Galter D, Mihm S, Droge W. Distinct effects of glutathione disulphide on the nuclear transcription factor kappa B and the activator protein-1. Eur J Biochem 1994;221(2):639–48.
[35] Nobel CS, Kimland M, Nicholson DW, Orrenius S, Slater AF. Disulfiram is a potent inhibitor of proteases of the caspase family. Chem Res Toxicol 1997;10(12):1319–24.
[36] Faiman MD, Dodd DE, Minor SS, Hanzlik R. Radioactive and nonradioactive methods for the in vivo determination of disulfiram, diethyldithiocarbamate, and diethyldithiocarbamate-methyl ester. Alcohol Clin Exp Res 1978;2(4):366–9.